Escola Superior de Tecnologia i Ciències Experimentals

Theoretical study of the effect of pressure on the structure and properties of GeSe

Final Degree Project

Author:

Rodrigo Más Herranz

Tutor:

Armando Beltrán Flors

June 2023

Index

1 Aim

The aim of this project is the theoretical study, using Crystal software, of the effect of the pressure on the structure and properties of GeSe

2 Introduction

GeSe is strongly anisotropic semiconducting van der Waals crystal isoelectronic to black phosphorus, with superior stability in air conditions. High optical absorption, good conductivity, and band gap ranging around 1,1 eV make this material suitable for various optoelectronic applications[1]

Figure 1: GeSe crystal

Germanium Selenide is a chemical compound of the group IV chalcogenides, these elements are an important class of functional compounds because they have a number of physical properties. Among these compounds, the simple 1:1 binary germanium selenide has very interesting attention. From GeSe it can be syntesized nanostructures, which make technological applications such as nanoscale photodetectors. GeSe is a prototypical IV-VI semiconductor.

To study the effect of pressure on the structure and properties of GeSe it is going to be used the programme Crystal in the UJI calculation center, and making use of density functional theory and Hartree-Fock method combinated with two different types of hybrids functionals to make the calculations, B3LYP and HSE06. It will be used hybrid functional that makes lower error in front of the experimental values.

GeSe exhibits interesting optical properties. It absorbs in the infrared region, specifically in the mid-infrared range. This property makes it suitable for use in optoelectronic devices, such as photodetectors and infrared sensors. GeSe can be deposited as thin films using various techniques, including thermal evaporation, sputtering, and chemical vapor deposition. These thin films find applications in electronic and optoelectronic devices due to their unique properties and compatibility with thin-film manufacturing processes.

- Uses of GeSe [2]:

    1. Optoelectronics:

       GeSe finds application in optoelectronic devices, as IR sensors, photodetectors, and other devices used in IR imaging and sensing applications.

    2. Phase Change Memory (PCM):

       GeSe is an essential material in PCM technology. It serves as the active material that undergoes reversible phase transitions, enabling the storage and retrieval of data in non-volatile memory devices.

    3. Thermoelectric Devices and Energy Harvesting:

       GeSe's favorable thermoelectric properties make it useful for thermoelectric generators, solid-state cooling systems and energy harvesting.
       It can efficiently convert waste heat into electricity or provide cooling in applications where traditional cooling methods may not be feasible or efficient. GeSe can be used to convert waste heat from industrial processes or other sources into electrical energy, contributing to energy efficiency and sustainability.

4. Thin-Film Electronics:

   GeSe can be deposited as thin films using various techniques such as thermal evaporation and chemical vapor deposition. These thin films can be integrated into thin-film electronic devices like thin-film transistors, solar cells, and other electronic components.

Overall, GeSe's unique characteristics make it valuable for optoelectronic devices, phase change memory, thermoelectric applications, thin-film electronics, and energy harvesting systems.

3 Calculation Methods

- **Hartree-Fock Method**

  First, it is interesting to explain that method required that the final computed field from the charge distribution to be "self-consistent" with the assumed initial field. Therefore the self-consistency was a requirement of the solution and hence the name. That said, the Hartree-Fock (HF) method used in Chemistry is an approximation method to determine or solve the wave function and the energy of many bodies interacting in the stationary phase (complying with Eq. 1) that is time independent.

$$|\Psi(r,t)|^2 = \Psi^*(r,t)\Psi(r,t) = \Psi^*(r)^{iEt/h}\Psi(r)e^{iEt/h} = \Psi^*(r)\Psi(r) = |\Psi(r)|^2 \quad (1)$$

  This method was developed by D.R. Hartree in 1927, a bit after the discovery of Schrödinger's equation. It is based on semi-empiric methods established by Bohr, such as the calculation of the energy of one state - for the Hydrogen atom - that is related with the main quantum number in the following way:

$$E = -1/n^2 \quad (2)$$

  Starting from this equation, the energy levels of multi-electronic atoms may be defined when taking into account that the shielding of inner electrons is not total and, then, there is a quantum defect (d). Doing this, the formula for the energy levels is approximated with the following one:

$$E = -1/(n+d)^2 \quad (3)$$

Once the equation is developed, it is considered that the whole nucleus is fixed with the exception of the electrons (Eq. 4) and a potential V is generated by the Born-Oppenheimer approximation that is considered as reference. Thus, this method uses a self-consistent potential (each electron moves in a potential created by the rest of the electrons) to convert a multi-electronic problem into multiple mono-electronic problems. In this way the Schrödinger's equation of one atom electronic state for N electrons per atom is got.

$$\Psi_{total} = \Psi electronic \otimes \Psi nuclear \tag{4}$$

The analytic solution for this equation has not been found because the term depends as much from the electron i as from the electron j. Another consideration performed when applying this method is that each solution is a linear combination of a finite number of base functions and, moreover, that each self-function is described by Slater's determinant, which for a system of N electrons is defined as:

$$\Psi(x_1, x_2, ..., x_N) = \frac{1}{\sqrt{N!}} \begin{bmatrix} x1(x1) & x2(x1) & ... & xn(x1) \\ x1(x2) & x2(x2) & ... & xn(x2) \\ .. & ... & ... & ... \\ x1(xn) & x2(xn) & ... & xn(xn) \end{bmatrix} \tag{5}$$

Thanks to this determinant, the following considerations are met:

- The result will be an anti-symmetric function and, therefore, the symmetric ones will be disregarded.
- Pauli's exclusion laws compliance is assured.

In theory to use Slater's determinant as the approximation of the electronic wave function is correct, but the exact wave functions cannot be expressed by means of this determinant, since the Coulombic correlation is not taken into account.
Therefore a different result to the exact solution of the Schrödinger's equation with the Born-Oppenheimer's approximation will be obtained and the difference between both will be the correlation energy.
Finally, to indicate that this method is solved by convergence with an iterative methodology that is the following one:

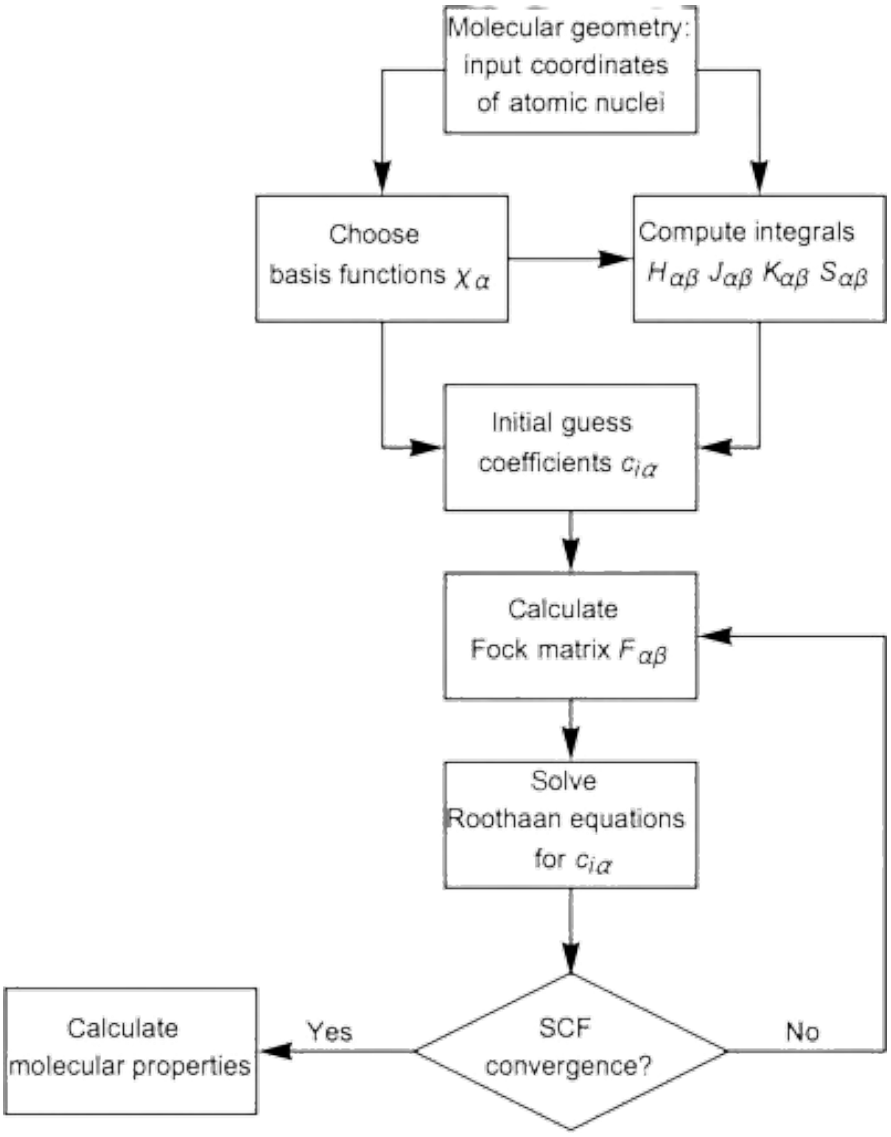

Figure 2: Simplified algorithmic flowchart illustrating the Hartree–Fock method

- **Density Functional Theory (DFT)** [3]

  It is a variational quantum-mechanical computational model, used to study the electronic structure, principally the basic state, of many-body systems (in this Project a multi-electronic compound is addressed). This model was started to be developed by L. Thomas and E. Fermi but the calculations were not established finally until 40 years afterwards, with P. Hohonberg, W. Kohn y L. Sham. It is presented as an alternative to the Schrödinger's equation solution and solved by means of the electronic energy minimisation versus the electronic density. The use of the electronic density versus the wave function makes it simpler and thus accessible to solve more complex systems since, instead of having 3N variables (in the case of the wave

function), only 3 variables are present. What is got with this method is, starting from a dependent on many-body problem, to get a non-dependent on single-body problem. In order to do it, the key variable is the electron density (p), which for a normalised is:

$$n(\vec{r}) = N \int d^3 r_2 ... \int d^3 r_N \psi^*(\vec{r}, \vec{r}_2, ..., \vec{r}_n)\psi(\vec{r}, \vec{r}_2, ..., \vec{r}_N) \tag{6}$$

This relationship can be reverted, which implies that for a given basic state density n0(r) there is a basic state wave function.

$$n_0 = (\vec{r}_1, ..., \vec{r}_n) \tag{7}$$

So 0 is an only functional of n0. And consequently the value expected of the basic state of an observable Rr is also a functional of n0. In particular, the energy of the ground state is a functional of n0.

$$E_0 = E[n_0] = <[n_0]> \tag{8}$$

Where the contribution of the external potential $\langle$n0$\rangle$ can be written in terms of the density of the basic state n0

$$V[n_0] = \int V(\vec{r}) n_0(\vec{r}) d^3 r \tag{9}$$

The functional Tn and Rrn are the called functional universal whereas Vn is the called no universal functional, since it depends of the system studied. As soon as system specified, have to minimise the functional.

$$E[n] = T[n] + Rr[n] + \int V(\vec{r}) n(\vec{r}) d3r \tag{10}$$

Assuming we have expressions of T[n] and Rr[n], the minimisation of n0 can be carried out. The problems that may appear when minimising can be solved if Lagrange's method is applied (non-determined multipliers), where it is considered that there is no interaction electron-electron and therefore that term is eliminated remaining
With all the previous calculations and assumptions, the Kohn-Sham's equations are solved for non-interactive systems. In the same way as for the Hartree-Fock's method, to solve the Khon-Sham's equation a nr is assumed. This will be the first term in the iterative method, where firstly Vs is calculated and then a new density is obtained fromVs. The process is repeated till the results converge.

- **Hybrid functionals**

The hybrid functionals are approximations that include the theories DFT and Hartree-Fock include in a way that an increased accuracy is got in the results for atomic energies, elastic constants or vibration frequencies. It is started to be used by 1993 introduced by A. Becke. Most of the hybrid functionals are formed by the linear combination of the exact exchange functional of Hartree-Fock :

$$E_x^{HF} = 1\frac{1}{2}\sum_{ij}\int\int \psi_i^*(\mathbf{r}_1)\psi_j^*(\mathbf{r}_2)\frac{1}{r_{12}}\psi_j(\mathbf{r}_1)\psi_i(\mathbf{r}_2)d\mathbf{r}_1 d\mathbf{r}_2 \tag{11}$$

And a number of exchange and correlation explicit density functionals. The parameters that determine the weight of each individual functional are adjusted by predictions of thermodynamic data either experimental or approximated.
There are several kinds of hybrid functionals, though in this project only B3LYP y HSE06 are going to be used due to, according to the bibliography, they provide better results for the calculations that will be carried out.

– **B3LYP** [4] [5]

The exchange-correlation functional B3LYP or Becke-3 parameters-Lee-Yang-Parr is applied using the following exchange-correlation functional:

$$E_{xc}^{B3LYP} = E_x^{LDA} + \alpha_0(E_x^{HF} - E_x^{LDA}) + \alpha_x(E_x^{CGA} - E_x^{LDA}) + E_c^{LDA} + \alpha_c(E_c^{CGA} - E_c^{LDA}) \tag{12}$$

The parameters used are: , and . Additionally and are approximations of generalised gradients (Becke 88 exchange functional and Lee-Yang-Parr correlation functional):

$$E_{XC}^{CGA}[n_\uparrow, n_\downarrow] = \int \varepsilon_{XC}(n_\uparrow, n_\downarrow, \nabla_\uparrow, \nabla_\downarrow)n(\vec{r})d^3r \tag{13}$$

Lastly, the parameter is referred to the Volsko-Wilk-Nusair's local-density approximation for the correlation functional:

$$E_{LDA}^{XC}[n] = \int \varepsilon_{xc}(n)n(\vec{r})d^3r \tag{14}$$

There are three parameters that are obtained from the precursor of this method, the B3PW91: Ionisation potentials, protonic affinity and total atomic energy.

– **HSE06** [6]

The exchange-correlation functional HSE (Heyd-Scuseria-Ernzerhof) uses the Gauss' error function applied to a shielded coulombic potential to calculate the energy exchange for improving the efficiency in the calculations:

$$E_{xc}^{wPBEh} = \alpha E_x^{HFSR}(\omega) + (1-\alpha)E_x^{PBESR}(\omega) + \\ + E_c^{LDA} + E_X^{PBELR}(\omega) + E_c^{PBE}$$

The parameters are: a (a parameter used to adjust the methods forming the HSE) with a standard value of 0.25 and w (variable parameter that indicates the short-range interactions) with a standard value of 0.2. ExPBE,SR, ExPBE,LR y EcPBE are parameters used in the functional Perdew, Burke, and Ernzerho (PBE) (different from the worked ones) and that indicate the components at different ranges and the correlation functional respectively. Finally ExHF,SR indicates the Hartree-Fock exact exchange functional of short-range.

- **Grimme's approximation**

The hybrid functionals provide very accurate results in the majority of the cases and due to that reason they are the most used currently. However, there are situations where they do not fit real values, as when by the method it is obtained that the structure "a" is more stable than the structure "b", but experimentally it has been demonstrated that the situation is just the contrary. To avoid this error Grimme proposed some empiric correction values for DFT method where dispersion of energy is considered.

An example where this approximation is needed to match the experimental and theoretical value is the Pnma, Cmcm and Fm-3m structures, which are different forms of the GeSe . In order to take into account van der Waals interactions, which can in fact play a significant role in this type of systems, the semiempirical Grimme extension of the standard DFT method (DFT+D) is an effective way of incorporating dispersion interactions, and it has proven its ability to provide reliable modeling of geometries and a better description of this type of interaction in metal oxides. Therefore, the empirical correction scheme to energy that considers the long-range dispersion contributions proposed by Grimme [7] and implemented by Bucko [8] for periodic systems was used. The basic strategy in the development is to restrict the density functional description to shorter electron correlation lengths scales and to describe situations with medium to large interatomic distances by damped terms, where denotes the dispersion coefficient for atom pair ij, and is the corresponding interatomic distance.[7]

- **Real and reciprocal spaces**

The concept of real space is intuitive since it is the one used daily. It is the place where objects are located and the events that happen have relative position and direction. In this real space it is possible to work with classic mechanics, which makes it ideal in the calculation for bodies of finite and measurable magnitudes. In contrast there are the infinite bodies, whose properties imply a big amount of calculations, many times not possible to be performed. For studying these bodies it was developed an idea that allowed the representation of them with finite magnitudes, the reciprocal space. The case dealt with in this project is based on a solid that is considered a periodic system of infinite atoms. For the calculation of some of its properties a series of mathematical operations is used, to get a group of imaginary points belonging to the reciprocal space, for crystals in 1,2 and 3D the Equation 15 (is the general condition for crystals in 1, 2 and 3 dimensions) is applied and The equation 16 is the reciprocal space for a crystal in 3D:

$$a_i b_j = 2\pi\delta_{ij} \tag{15}$$

$$\vec{k} = (\frac{2\pi m}{a_1}, \frac{2\pi n}{a_2}, \frac{2\pi q}{a_3}) \tag{16}$$

Where "a" represents the vectors generators of the direct net:

$$\vec{R} = m_1\vec{a_1} + m_2\vec{a_2} + m_3\vec{a_3} \tag{17}$$

And "b" the ones generating the reciprocal one:

$$\vec{k} = v_1\vec{b_1} + v_2\vec{b_2} + v_3\vec{b_3} \tag{18}$$

Once the set of points of the reciprocal space is got, calculations are easier. There are 14 Bravais lattices and 230 space groups, each one has one different first Brillouin zone, this is the primitive reciprocal lattice. In this study there are going to be studied the Pnma (space group (spg) 62), Cmcm (spg 63) and Fm-3m (spg 225).

- **Equations of State EOS**

The thermodynamic equations of state are mathematical expressions that relate state variables which define the physic conditions of a compound as pressure, temperature, volume or the internal energy.

There are a lot of equations of state, each one allows to define one or more variables and furthermore they change with each different system. The equations that are going to be use in this project are Murnaghan equation and Birch-Murnaghan equation. These two equations show the relation between the volume of a system and the applied pressure. It bases on Boyle law but adds two variable parameters: the inverse of compressibility module or Bulk modulus.

  - Murnaghan equation [9]:

$$P = \frac{K_0}{K_0'}((\frac{V_0}{V})^{K_0'} - 1) \tag{19}$$

  - 3rd order Birch-Murnaghan equation [9]:

$$P = \frac{3}{2}K_0(r^{7/3} - r^{5/3})[1 + \frac{3}{4}(K_0' - 4)(r^{2/3} - 1)] \tag{20}$$

In equation 19:

$$r = V/V_0; \frac{1}{\beta} = K = -V(\frac{dP}{dv})_T; K' = \frac{dK}{dP} \tag{21}$$

- **Grüneisen Parameter**

This parameter presents, for a crystal net, the effect in vibration frequencies (w) with a volume variation due to a decrease of pressure. In this study althought there are two diferent equations which describes this parameter, it is going to be used the microscopic equation.

$$\gamma = \frac{1}{w_0}\frac{dw}{dP} \tag{22}$$

When the parameter is negative, it indicates that the structure becomes unstable dynamically. Using this parameter it can be studied the dynamic stability.

- **Band structure**

To introduce the concept of band structure, firstly the presentation of the theory of bands is needed. By this theory, the electronic structure of a compound is described, an GeSe crystal in this project , as a structure of energy bands. This is possible since the orbitals of the atoms when joining to make a molecule overlap, producing a discreet number of molecular orbitals, each one with its own energy. When the crystal has a big number of atoms, the number of orbitals of valence is also big and, as the energy difference is so low, the energy levels nearly overlap forming continuous bands. Among bands, empty breaches are created, due to the absence of orbitals in such energies (these breaches will be formed whatever the number of atoms may be).

The band occupied by the most external electrons of the atom (the ones in the last

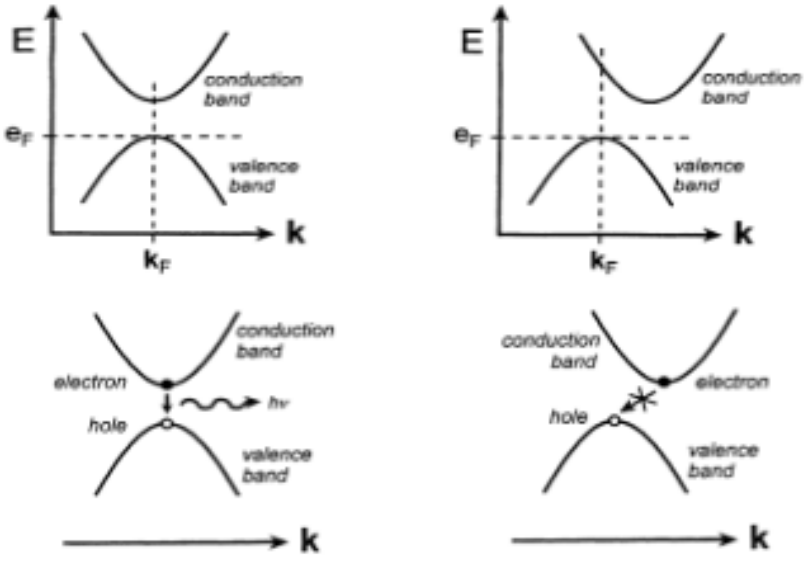

Figure 3: Direct and Indirect bandgap [10]

layer) will be the valence band. These electrons are used to make bonds but they cannot be used for electrical conduction. The conduction band is the first one that presents free electrons and the band that produces electrical conduction, since these electrons are not linked to the atoms anymore and, therefore, they can move along the crystal.

Another concept that must be considered is the one called in this work, the maximum of the valence band, the Fermi's energy or level. There is another definition of

this concept widely used in solid-state physics, defined as the average between the two bands, with the conduction band that is located in the upper part of the Fermi's energy and the valence band located in the lower part.

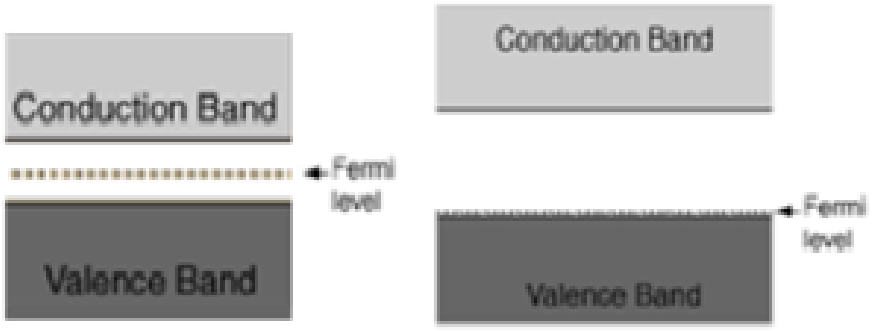

Figure 4: Two definitions of Fermi's Energy

The minimum separation between the conduction band and the valence band is called band gap and there is no energy levels in this zone. Its value is measured taking the lowest energy in the conduction band and deducting the value of the highest energy in the valence band. These values are obtained from some of the k points in the first zone of Brillouin, in such a way that if the vector representing the maximum of the valence band and the vector representing the minimum of the conduction band are the same one, a direct gap will be given, meanwhile if different k points represent the maximum and the minimum, the gap will be indirect. See figure 3.
Besides, is useful to say that when the compound is a metal, there is not any separation between the valence and conduction bands, these are overlapping. In the semiconductors the gap is above 0 and 3 eV.

4 Computational Details

This project was doing using UJI computing center with Crystal [11] program. This program helps us to make calculations related with the solid state chemistry in 0 (molecules), 1 (linear polymers), 2 (crystal surfaces or films) and 3 dimensions (crystals). It uses as a base the calculation methods, crystallographic bases and hybrid functionals that has been introduced before. Crystal17 takes the crystal systems as periodic, this consideration allows the simplification and the speed-up of all the calculations.
To do the calculations the program ask for four different kind of archives that are the bases for almost all the calculations of this project. The four archives are, an INPUT, an OUTPUT, and fort.9 and fort.34,

- INPUT

  This archive contains the following structure for the dada: First of all there are one line for the title, the next lines indicate the type of calculation that is going to be done and the conditions (in this case the value of the pressure) and other parameters. Then comes the crystallographic bases, the order doesn't matter. And lastly comes the step, the functionals and another values as modes of work that can be found in the manual. This archive is the base to make the calculations.

- OUTPUT

  This archive contains the results of the calculations. First of all the output shows the information related to the process to make the calculations (time, steps, type of calculations, parameters set in the input). When this first part ends a resume of the equations that has been solved and all the calculation are shown. Lastly the iteration process can be found with the final solution at last.

- fort.34

  Those archives are given by crystal as a complement of the optimization processes. Fort.34 gives additional information of the geometry of the structure and serve as complement in subsequent calculations.

- fort.9

  This archive contains information related to the electronic structure that can be used in different programs (Xcrysden, crysplot or origin) to obtain the bands diagram and a band gap.

5 Previous Data

Before beginning the experimental calculations it must be explained which structures are going to be studied for GeSe under pressure.
According to another investigations and papers which study the effect of increasing pressure or temperature in the GeSe and others chalcogenides compounds. These structures are orthorhombic Pnma (spg 62), orthorhombic Cmcm (spg 63) and cubic Fm-3m (spg 225).

- Pnma structure (spg 62)

  The structure has been obtained by the use of Diamond software [12]:

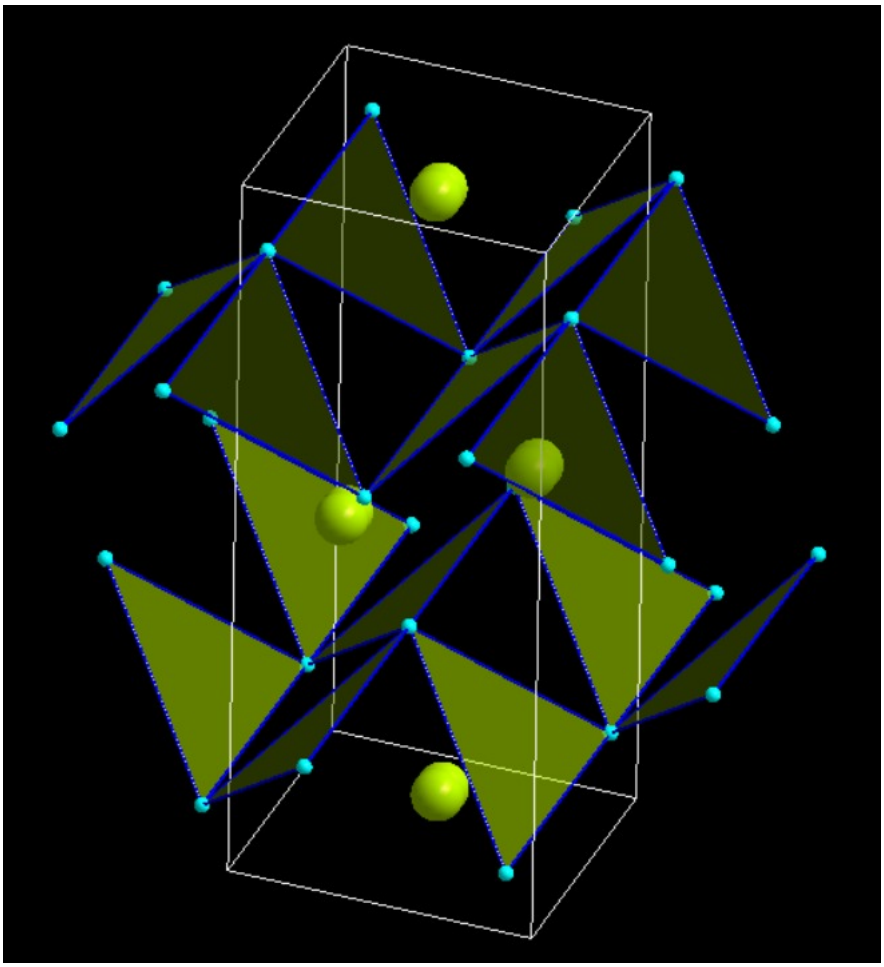

Figure 5: Structure of Pnma

Green atoms are Germanium Blue atoms are Selenium

This is a orthorombic structure, space group 62, Pnma. The latticce parameters are a=10.9208 Å b=3.8708 Å and c=4.4075 Å.

Seeing this Figure the Germanium is surrounded by one atom of Selenium at 2.5665 Å and by two atoms of Selenium at 2.5770 Å. The coordination of Germanium around Selenium is three, so, this is a layer structure. There are also two other atoms of Selenium at 3.3387 Å and it could be considered a very irregular five fold coordinatio. The coordination of Selenium is also three. Selenium is surrounded by one atom of Germanium at 2.5665 Å, and there are two other atoms of Germanium at 2.5770 Å.

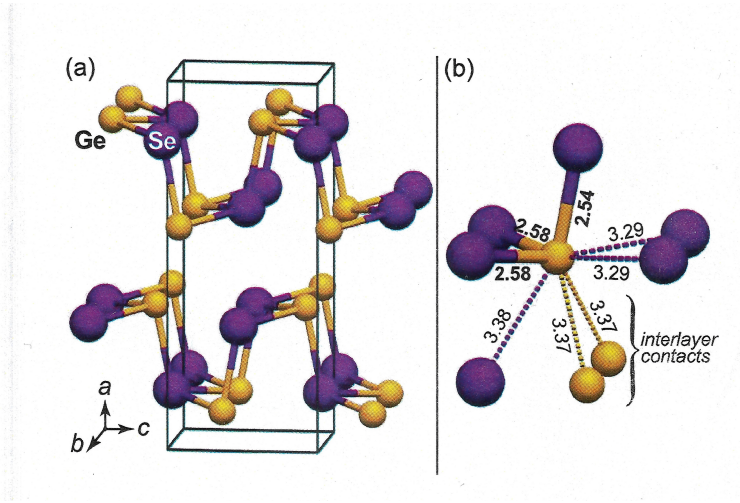

Figure 6: Ball and stick Pnma structure

It is also represented the structure of Pnma taken form [13] (a) Balls-and-sticks representation. Ge atoms are drawn as smaller, orange spheres, and Se atoms are larger and in purple. (b) Close-up of the coordination environment surrounding one of the germanium atoms. Both species are interchangeable in principle. The closest covalent Ge-Se bond distances are given in boldface; the next-nearest Ge-Se bonds, drawn with dashed lines, allude to the relationship with the rocksalt structure. There are also two Ge-Ge bonds in the second coordination sphere.

- CmCm structure (spg 63)

  The structure has been obtained by the use of Diamond software:

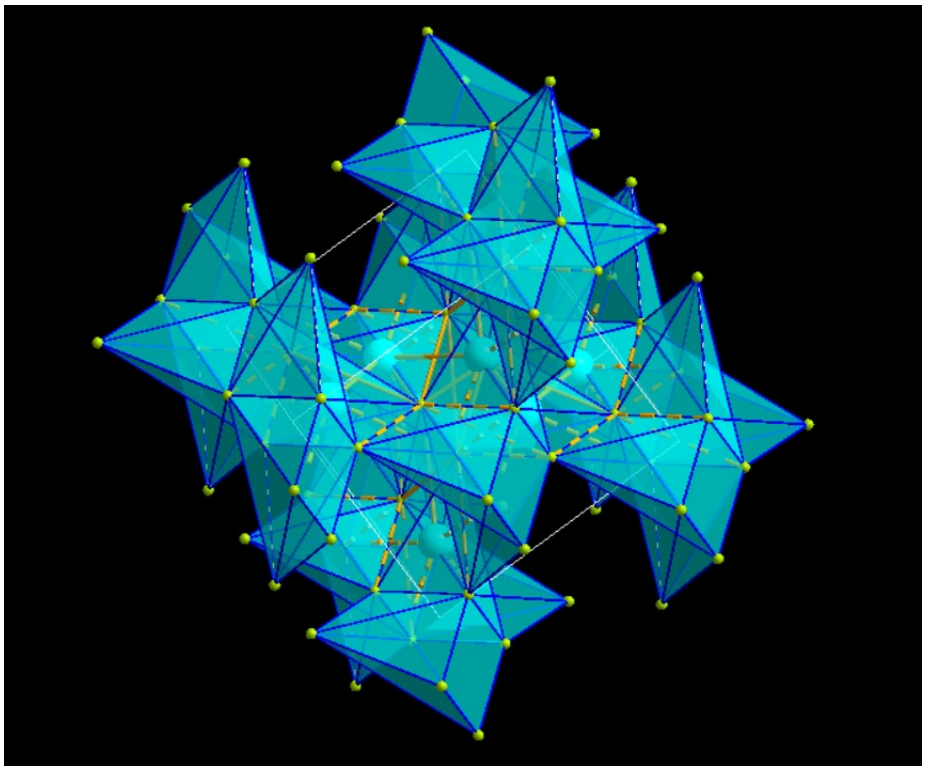

Figure 7: CmCm structure

This structure is also orthorombic structure, space group 63, CmCm, the lattice parameters are a=5.3100 Å b=12.4850 Å c=4.6500 Å.

This structure is caracterized because the coordination is 5 both for Se and Ge

- Fm-3m structure (spg 225)

  The structure has been obtained by the use of Diamond software:

  This structure is a cubic structure, space group 225, Fm-3m, the lattice parameters are a=b=c=5.5040 Å.

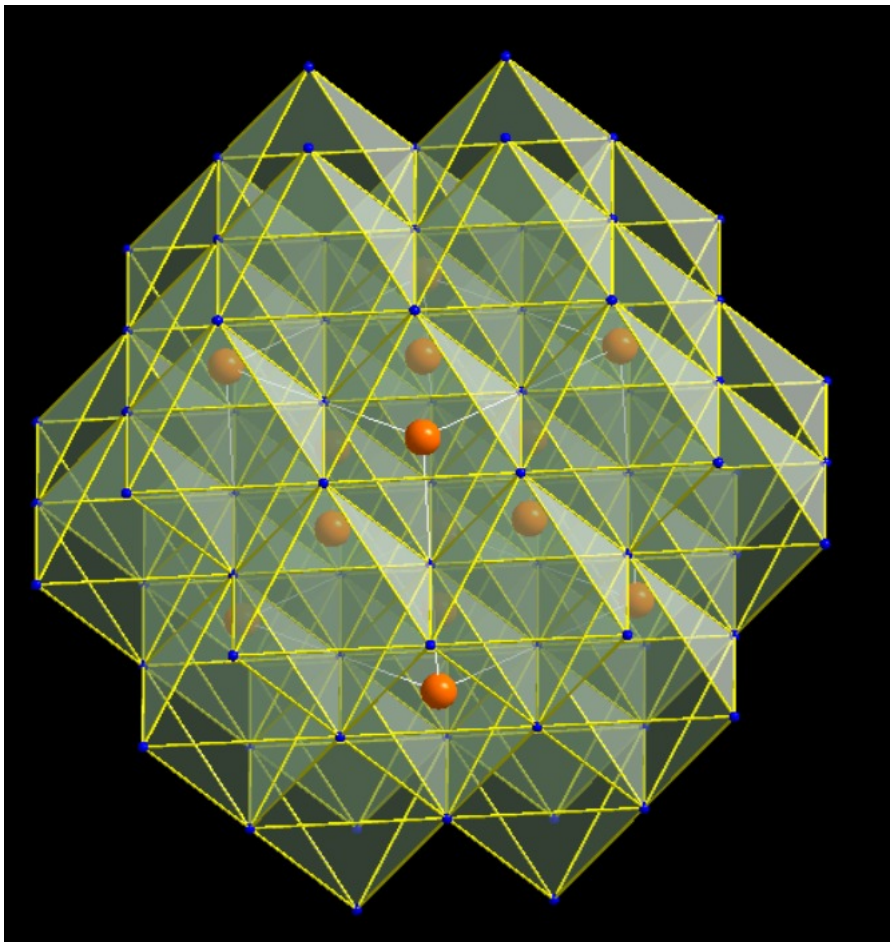

Figure 8: Fm-3m structure

Red atoms are Germanium and Blue atoms are Selenium.

Seeing this Figure, Germanium is surrounded by 6 atoms of Selenium at 2.7379 Å, and the Selenium is surrounded by 6 atoms of Germanium at 2.7379 Å too. The coordination, as the germanium is surrounded by 6 selenium atoms, as deformed octahedra.

6 Stability criteria

A structure presents an energy minimum if the first derivate of the energy respect to the energy is equal to zero. In order to determine which structure presents more stability at a determinate pressure we must study three criteria.

- An energy minimum

  The necessary condition for a structure to be an energy minimum is that the first derivate of the energy front of q (the coordinates) becomes zero. The coordinates are the ones that are going to be optimized. These coordinates are related to the volume of the structure that will be affected as the pressure changes

- Second derivative: Dynamic criteria

  To ensure that the optimized structure is a true minima it is necessary that all the second derivatives of the energy with respect to the coordinates are greater than zero.

$$\omega = \frac{d^2E}{dq^2} > 0 \tag{23}$$

  Besides, as the frequency values are equal to the second derivate of the energy front q, this condition is equivalent to that all the frequency vibrations are positives. if the frequecy values increases with the pressure, the structure is stable. If the vibration frequency has decreased means that there is an instability and the structure can be transformed in other one.

- Mechanical stability

  The mechanical stability for the GeSe phases was analyzed by calculating the corresponding symmetrized elastic constant at several pressures. From these elastic constants, we applied the Born criteria [14] for the confirmation of the stable structure [15]

  Firstly, the elastic constants are been calculated. Furthermore, the generic mechanical stability conditions for crystals and Born criteria [10] for each structure will be studied. In the case of Orthorhombic systems (Pnma and CmCm in our case) the stiffness matrix for an orthorhombic crystal has the following form, with 9 constants and no relatonships between them:

$$Cortho = \begin{bmatrix} C11 & C12 & C13 & & & \\ . & C22 & C23 & & & \\ . & . & C33 & & & \\ & & & C44 & & \\ & & & & C55 & \\ & & & & & C66 \end{bmatrix} \tag{24}$$

The following Born criteria for an orthorhombic system:

$$C_{11} > 0; C_{11}C_{22} > C_{12}^2 \tag{25}$$

$$C_{11}C_{22}C_{33} + 2C_{12}C_{13}C_{23} - C_{11}C_{23}^2 - C_{22}C_{13}^2 - C_{33}C_{12}^2 > 0 \tag{26}$$

$$C_{44} > 0; C_{55} > 0; C_{66} > 0 \tag{27}$$

The conditions of the Pnma and CmCm structures are both equal to the Equation 18, 19 and 20, and the matrix is both the same.

If the structure is a cubic crystal system:

$$Ccubic = \begin{bmatrix} C11 & C12 & C12 & & & \\ . & C11 & C12 & & & \\ . & . & C11 & & & \\ & & & C44 & & \\ & & & & C44 & \\ & & & & & C44 \end{bmatrix} \tag{28}$$

The following Born criteria for an cubic system:

$$C_{11} - C_{12} > 0; C_{11} + 2C_{12} > 0; C_{44} > 0 \tag{29}$$

7 Geometry and Energy

- In addition to the elastic stability criteria, more also studies are also going to be made to ensure the results are reliable. It is going to be stydied the Equations of State (EOS). This is being based on third order Birch-Murnaghan equation of state for energy and and also on the equations Pressure vs Volume (see in page 11, equations 19 and 20)

  Murnagham Equation

$$E(V) = E_0 + (\frac{K_0 V}{K_0^{'}})(\frac{r^{K_0^{'}}}{(K_0^{'}-1)} + 1) - \frac{V_0 K_0}{K_0^{'}-1} \tag{30}$$

  3rd order Birch-Murnaghan equation

$$E(V) = E_0 + \frac{9}{4}K_0 V_0(\frac{1}{2}r^{4/3} - r^{2/3}) + \frac{9}{16}K_0 V_0(K_0^{'}-4)(r^2 - 3r^{4/3} + 3r^{2/3}) \tag{31}$$

  Moreover the band structures of each structure will also be made. Once this band structures will be made it will be possible calculate and determine the Band Gap Energy and if it is direct or indirect.

8 Results

- HYBRID FUNCTIONALS

  In the case of this study, the hybrid functional that will be used, is which produces the least error compared to the experimental data of the Pnma GeSe orthorhombic structure.

Table 1: Table 1. Results of B3LYP and HSE06

	a (Å)	**b (Å)**	**c (Å)**
experimental	10.9208	3.8708	4.4075
HSE06-D3	10.7990	3.8424	4.4142
B3LYP	10.9672	3.8632	4.4984

Table 2: Table 2. Results of Volume, error Volume and Hartree Energy of B3LYP and HSE06

	volume (Å3̂)	**error volume (Å3̂)**	**Eg (eV)**	**Error Eg (eV)**
experimental	186.32	-	1.1	-
HSE06-D3	183.16	3.15	1.21	0.11
B3LYP	190.59	4.27	1.78	0.68

According to the results, the hybrid functional HSE06-D3 will be used to make the calculations to discuss the effect of pressure on the GeSe. The error of the volume as well as the energy gap are lower in HSE06-D3 than in B3LYP.

The same occurs with the difference between the Hartree energy of the functional hybrid HSE06-D3 and B3LYP. It is smaller when is used HSE06-D3.

- GEOMETRY AND ENERGY

  Figure 9 is done using the Gibbs free energy values in all the pressure range. By this plot is check if there are any intersection between the structures. This graph represents the difference of the Gibbs free energy for the three studied structures of GeSe with respect to that of the Pnma structure.

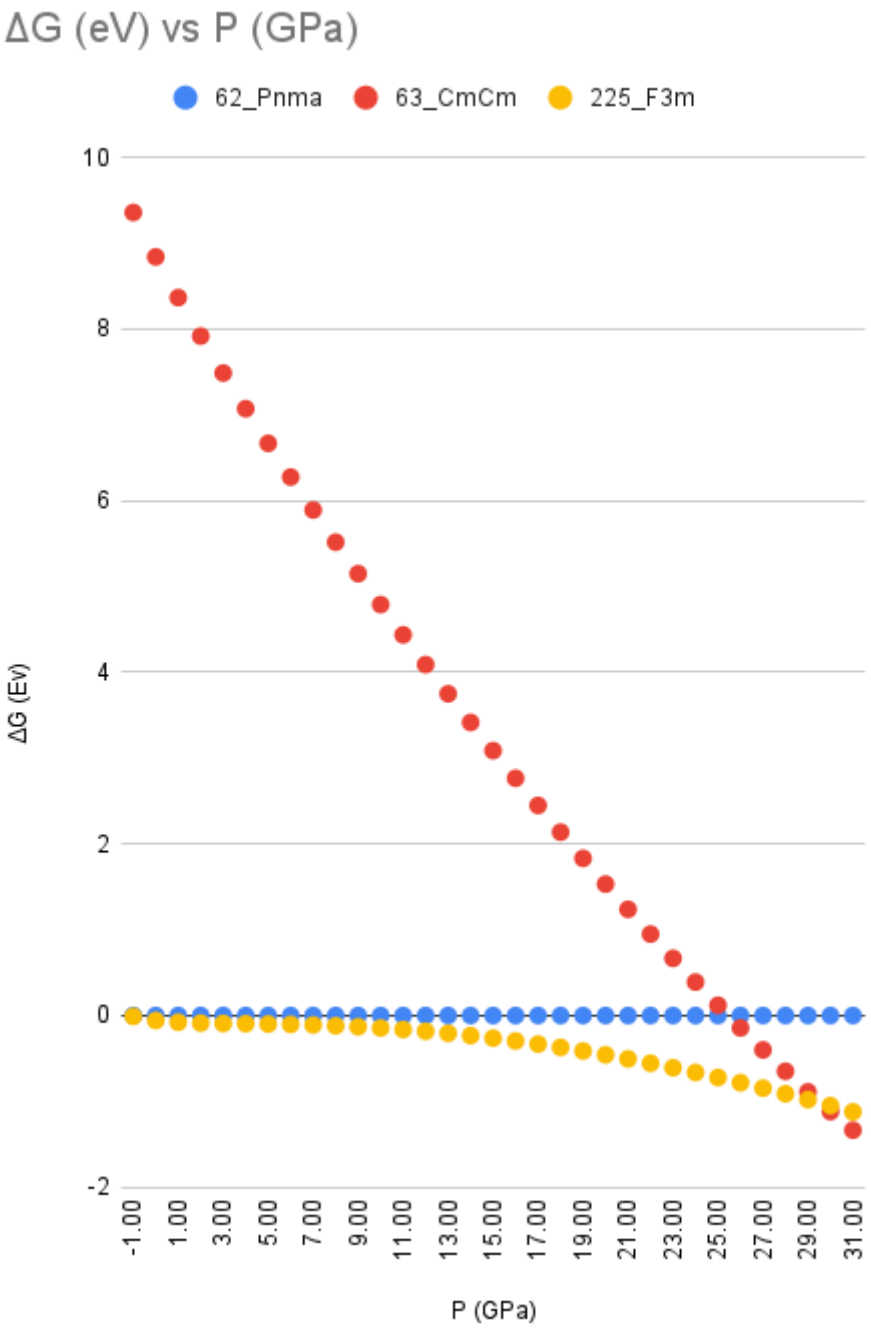

Figure 9: Variation of Gibbs free energy vs Pressure

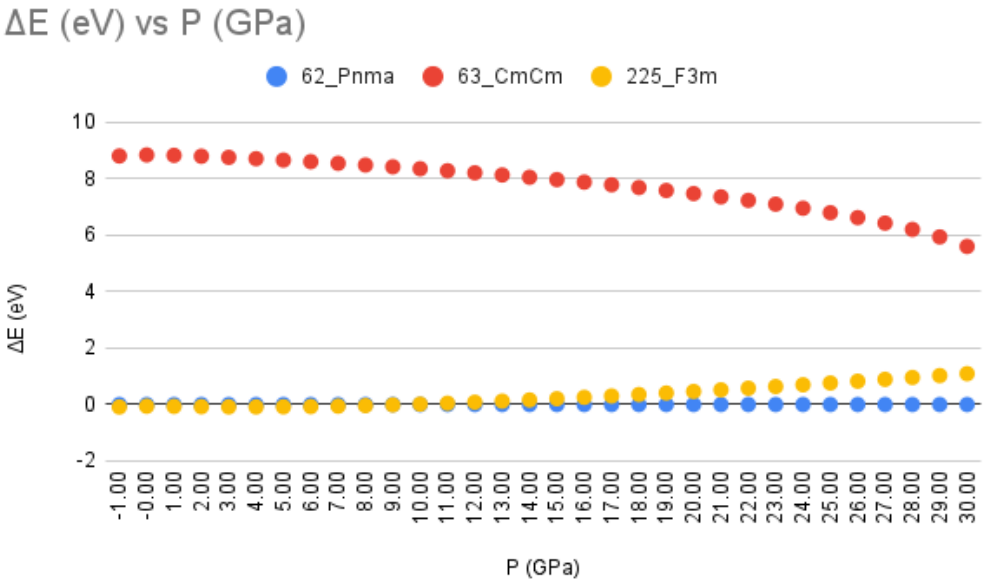

Figure 10: Variation of internal energy vs Pressure

In this graphs is observed that at zero pressure the structure that is more stable in its fase is the yellow line, it corresponds to the cubic structure because the value for each pressure of Gibbs free enthalpy is the lowest. But a cubic structure is more stable at lower pressure than the Pnma and CmCm, it is due to is only accessible at high temperatures, and probably kinetics impedance.[16]
Moreover in the Figure 9 is observed that at 27GPa there is a crossing between the blue and red lines, this may indicate that it is a phase change between structures. It changes from a orthorhombic(Pnma) to a CmCm structure.

At lower pressures the Pnma structure is more stable than the CmCm structure. According to the Figure 9, the calculations predict the possibility of the phase transition from the orthorombic phase Pnma to phase CmCm at a pressure about 27 GPa.
Respect to the Figure 10, the internal energy of cubic phase is less stable up to 10 GPa and the internal energy of CmCm is less stable than the Pnma structure.

- It has been also studied the evolution of the lattice parameters of the orthorhombic (Pnma structure) as the pressure increases.

ao (Å)	10.7990
bo (Å)	3.8424
co (Å)	4.4142

P (GPa)	**a (Å)**	**b (Å)**	**c (Å)**	**a/ao**	**b/bo**	**c/co**
0	10.7990	3.8424	4.4142	1	1	1
5	10.2583	3.7587	4.0421	0.9499	0.9782	0.9157
10	10.0971	3.7091	3.7091	0.9350	0.9653	0.8403
15	9.9847	3.6643	3.8140	0.9246	0.9536	0.8640
20	9.8767	3.6269	3.7463	0.9146	0.9439	0.8487
25	9.7628	3.6577	3.5757	0.9040	0.9519	0.8100
30	9.6854	3.6222	3.5397	0.8969	0.9427	0.8019

Table 3: Lattice parameters at different pressures

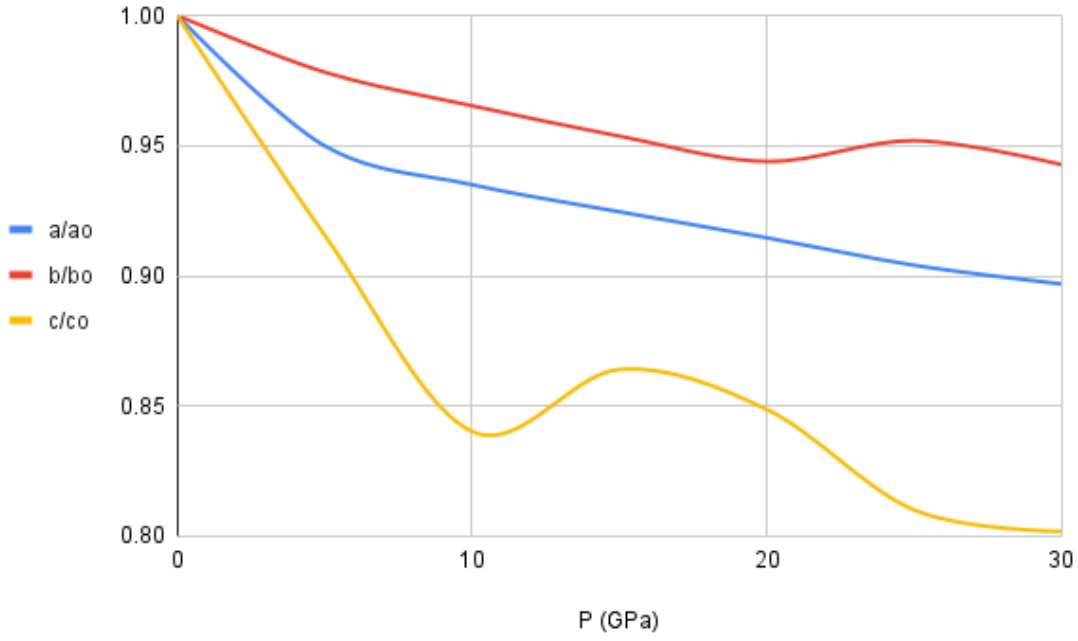

Figure 11: Evolution of lattice parameters when pressure increases

Seeing this, the parameter c/co is the one that varies the most when the pressure increases.

All the parameters decreases with the pressure, so the volume values decrease under pressure too.

- MECHANICAL STABILITY

P (GPa)	**K (GPa)**	**G (GPa)**	**E (GPa)**	**v**
0	70.87	32.06	83.59	0.303
5	77.03	54.85	132.98	0.212
10	88.03	63.11	152.81	0.211
15	112.25	75.34	184.71	0.226
20	135.18	85.22	211.28	0.240
25	164.35	105.79	261.30	0.235
30	182.81	119.37	294.10	0.232

Table 4: Modulus data for Pnma structure

In this table, K means Bulk modulus [17], G is the Shear modulus, E is the Young modulus and v is the Poisson ratio. All of them are measured in GPa except Poisson ratio that is adimensional. This calculations are made according Hill method [18] (it is the arithmetic average between Voigt and Reuss methods)

The bulk modulus or compressibility modulus of a material measures its resistance to uniform compression and, therefore, indicates the increase in pressure required to cause a unit decrease in a given volume.
Also it is shown the evolution of Poisson Coefficient increasing pressure.

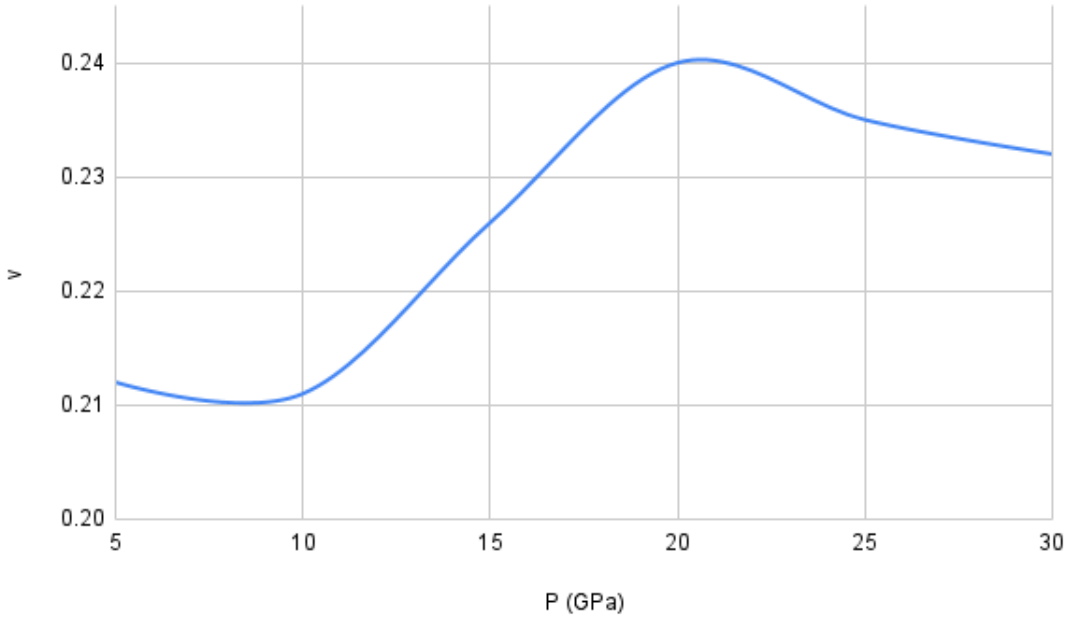

Figure 12: Poisson coefficient vs Pressure

It can be determined that at pressures highers tan 20 GPa the Poisson Coefficient decreases.

Seeing the table in the annex is determined that the conditions are met It is also studied the generic elastic stability conditions for each pressure. In all of them the conditions are accepted.

Besides, the elastic stability conditions of orthorombic Pnma and Cmcm, and cubic Fm-3m structures have been studied, and all structures fulfill the Born at ambient pressure criteria.

The table the most important elastic which contains each elastic constants are in the annex.

It is observed that at zero pressure the orthorhombic structure Pnma is stable at P=0 and for all pressure (tables in the Annex)

124.081	40.714	41.940	0.000	0.000	0.000
0.000	129.392	70.883	0.000	0.000	0.000
0.000	0.000	87.565	0.000	0.000	0.000
0.000	0.000	0.000	54.385	0.000	0.000
0.000	0.000	0.000	0.000	28.835	0.000
0.000	0.000	0.000	0.000	0.000	28.038

Table 5: Elastic constants at 0 GPa of Pnma

In the following table at pressure 0, is demonstrated that Fm-3m structure is stable.

174.308	30.087	30.087	0.000	0.000	0.000
0.000	174.308	30.087	0.000	0.000	0.000
0.000	0.000	174.308	0.000	0.000	0.000
0.000	0.000	0.000	-6.417	0.000	0.000
0.000	0.000	0.000	0.000	-6.417	0.000
0.000	0.000	0.000	0.000	0.000	-6.147

Table 6: Elastic Constants at 0 GPa of Fm-3m

CmCm strucutre is also stable at 0 GPa seeing the tfollowing table:

129.306	2.936	54.296	0.000	0.000	0.000
0.000	131.117	-5.204	0.000	0.000	0.000
0.000	0.000	119.686	0.000	0.000	0.000
0.000	0.000	0.000	11.024	0.000	0.000
0.000	0.000	0.000	0.000	111.006	0.000
0.000	0.000	0.000	0.000	0.000	33.201

Table 7: Elastic Constants at 0 GPa of CmCm

- FREQUENCIES

To study the geometry and the energy of the structure is possible to rely on a vibrational frequency analysis. It is based within harmonic approximation.

	Pressure (GPa)				
Raman Modes	**0**	**5**	**10**	**15**	**20**
B2g	48.54	58.37	60.76	61.22	59.39
Ag	46.49	59.10	62.42	63.58	63.70
B1g	86.27	85.34	86.22	87.25	88.90
Ag	94.08	99.40	106.30	101.06	95.53
B3g	98.32	109.56	108.23	113.84	118.69
B3g	106.36	117.48	133.61	147.71	158.93
B2g	156.64	173.14	172.10	167.39	160.05
Ag	168.31	199.42	196.62	192.01	188.07
B1g	183.65	201.47	211.51	218.20	222.39
B3g	205.45	215.06	218.21	220.44	223.73
Ag	206.63	226.82	243.71	247.23	249.91
B3g	232.92	243.72	245.58	256.58	270.59

Table 8: Vibrational frequencies for each Raman mode at different pressure

Besides, studying the Gruneissen parameter, according to the Table 4, in the mode B2g at 15GPa there are a drop in the frequency. In the mode Ag at 15 GPa there is a drop in the frequency too. And in the case of the B2g mode, at 10 GPa there is also a drop in the frequency. In the mode Ag at 10 GPa the frequency decreases too. These variations in the frequency cause the Gruneissen becomes negative and this facts indicates that the structure becomes unstable. This could lead to a phase change.

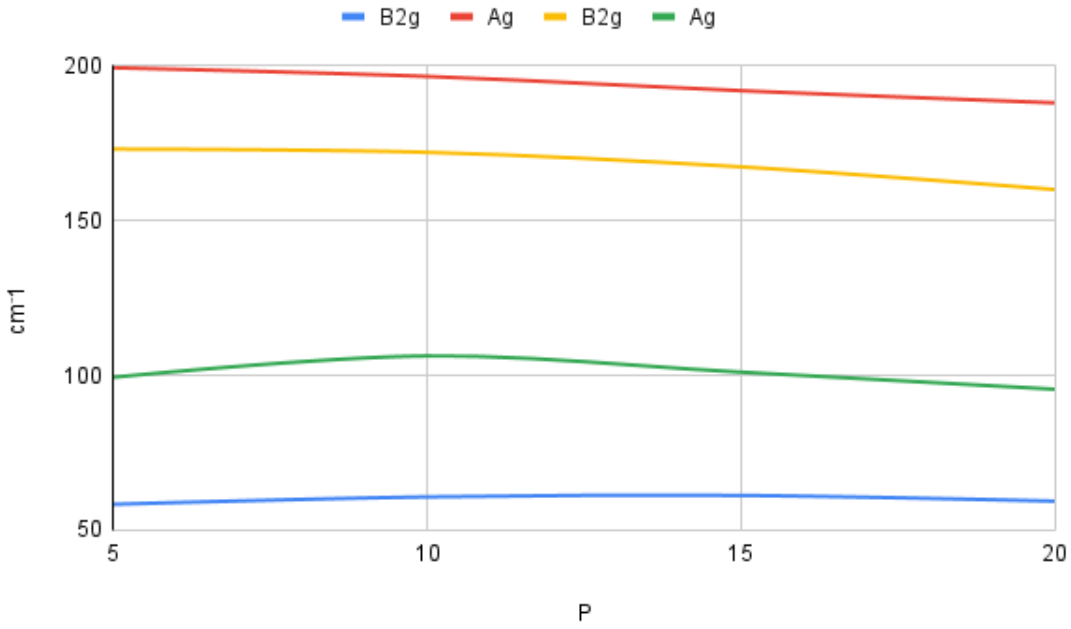

Figure 13: RAMAN frequencies vs Pressure

This graph shows the decrease of the active frequencies in Raman modes B2g, Ag, B2g and Ag (modes in which the frequency decreases), with the pressure, and passing from positive to negative slopes indicates that Gruneisen parameter becomes negative and the structure becomes unstable.

- BAND STRUCTURE

The obtained files fort.9 of each pressure are used to get all the different band structures. To do it is necessary a specific software, the Xcrysden programm [19], which allow the transformation of the fort.9 values into a band structure by calculations, related on the first Brillouin zone k points and vectors that link those.[20]
If the band structure evolution is studied, irregularities can be detected. The most important irregularities that can be found is the change of the band gap type, from direct to indirect or vice versa and a change in the band gap values.

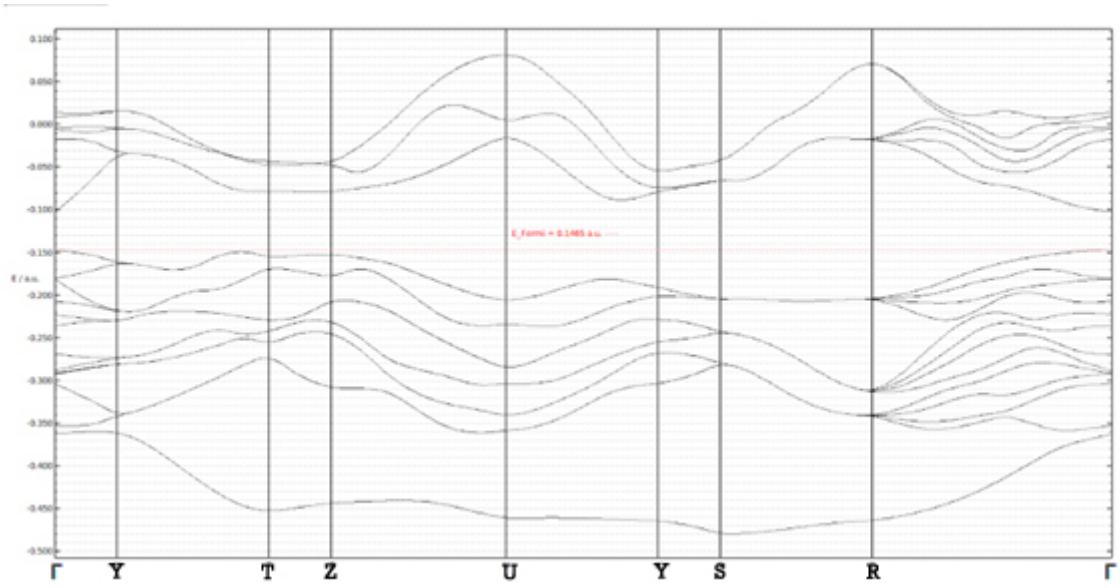

Figure 14: Band structure of Pnma

The gap is direct at Gamma (0,0,0) (two blue points marcked in the graph)

In the case of Cmcm structure:

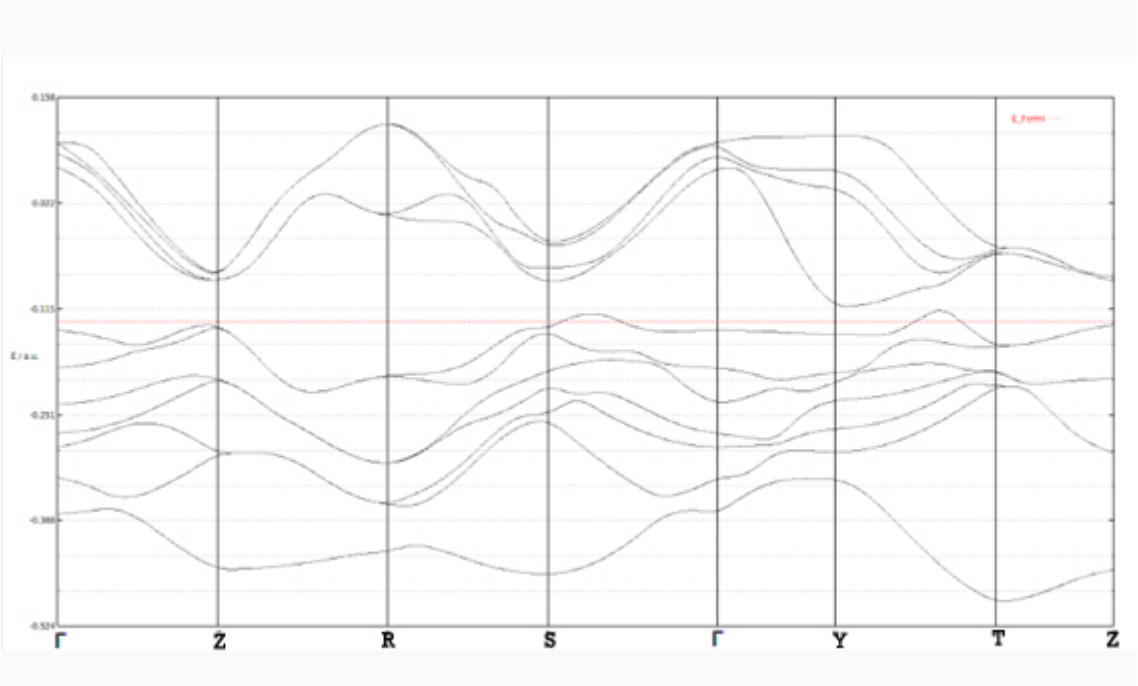

Figure 15: Band structure of Cmcm

The top of the valence band is found at a point between Y ($\frac{1}{2}$,$\frac{1}{2}$,0) and T ($\frac{1}{2}$,$\frac{1}{2}$,$\frac{1}{2}$), this being H with coordinates ($\frac{1}{2}$,$\frac{1}{2}$,alpha) The GAP is indirect and its value is given by the difference between the points Y and T. This difference is 0.4813 eV This value

coincides with the energy of indirect GAP which is 0.4815 eV

Finally in the case of Fm3m structure:

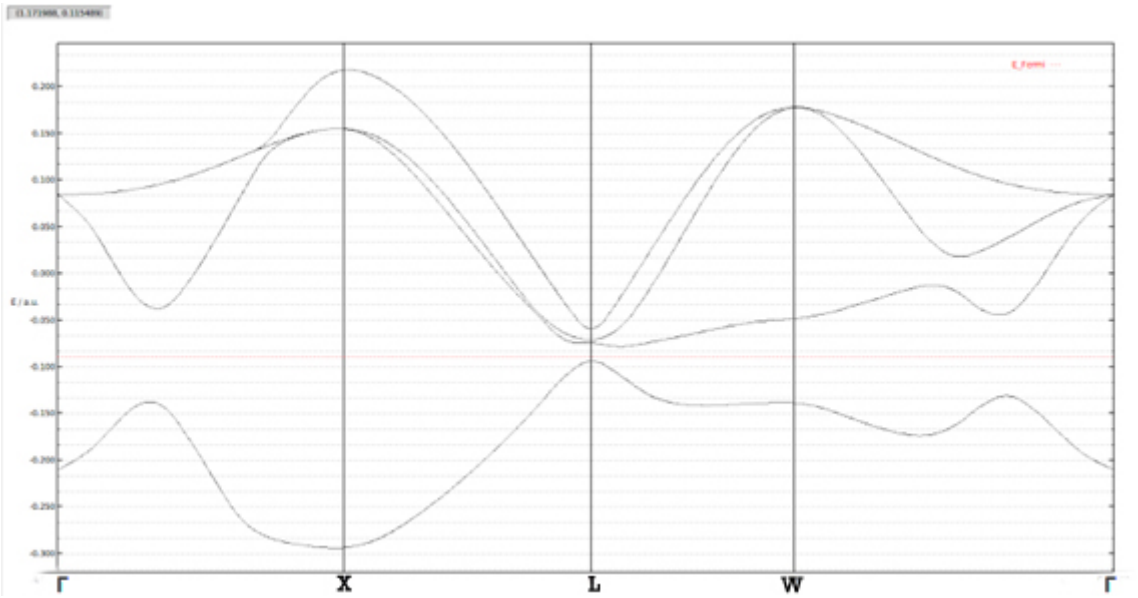

Figure 16: Band structure of Fm3m

The top of the valence band is found at point L, with coordinates ($\frac{1}{2}$,$\frac{1}{2}$,$\frac{1}{2}$) The GAP is direct and its value is 0.4129 eV The lowest value of the virtual band is at point Q, between point L ($\frac{1}{2}$,$\frac{1}{2}$,$\frac{1}{2}$) and W (1/2,1/4,3/4) of coordinates ($\frac{1}{2}$,$\frac{1}{2}$-alpha,$\frac{1}{2}$+alpha) The GAP is direct at point L

In all of this figures the blue points that represents de GAP are the top of the valence bands (for the lower point) and the bottom of conduction bands (for the upper point)

The effect of pressure to the Energy of Band Gap.

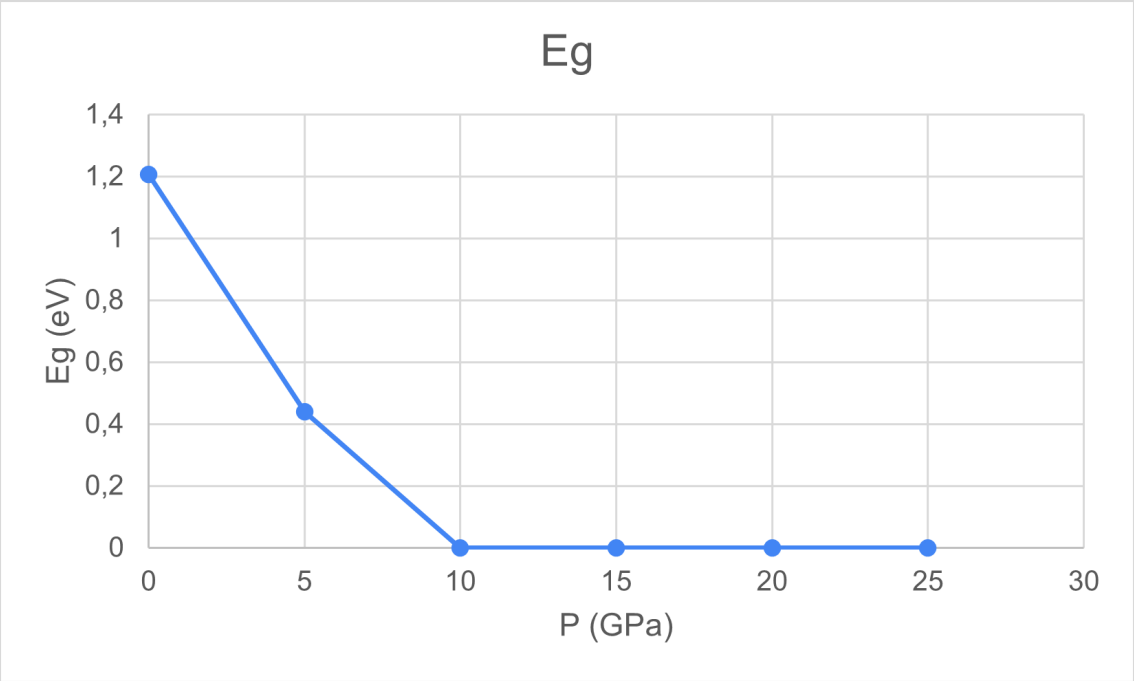

Figure 17: Band Gap vs Pressure

It may be commented that when passing from 5 to 10 GPa, the band gap decreases and this structure of GeSe becomes conductive up to 10 GPa.

9 Conclusions

As conclusions of this work on the theoretical study of the effect of pressure on the structure and properties of GeSe, we can say first of all that of the two functional structure and properties of GeSe, we can say in the first place that of the two functional hybrids chosen for the study, HSE06 has been used, since it has the least error the HSE06 has been used since it is the one that gives the least error with respect to the experimental data.

Regarding the stability of the structure, it can be observed that from 0 GPa to 27 GPa the structure with the more stability, without taking into account the cubic structure with the highest stability due to kinetic impedance factors and temperature, is Pnma structure, but the Pnma structure above 27 GPa suffers a phase change to CmCm structure.

As for the frequency analysis, a tendency is also observed that at higher pressure the structure tends to be unstable. In the case of the Pnma structure, this has been studied based on Gruneisen parameter. The Gruneisen parameter which, as the frequency decreases with pressure,becomes negative. It indicates that the structure is becoming unstable and it can be dueto a phase change.

The three structures studied show mechanical stability at ambient pressure (0 GPa) and Pnma is also mechanically stable throughout the range of pressures studied (0-30 GPa).

Regarding the study of the band structure, looking at the value of the Band Gap decreases with respect to the pressure, when passing from 5 to 10 GPa the structure becomes conductive up to 10 GPa.

As a final conclusion we can say that by applying a pressure lower than 10 GPa to the Pnma structure, without increasing the temperature (which can overcome the kinetic barrier and make it transits to the cubic structure) the GeSe decreases its gap being still semiconductor, which can be beneficial for its computer applications.

10 Bibliography

References

[1] Liu, S.-C., Mi, Y., Xue, D.-J., Chen, Y.-X., He, C., Liu, X., Hu, J.-S., Wan, L.-J., Adv. Electron. Mater. 3, 1700141, 2017.

[2] Kim, Y., Choi, IH. Optical and electrical properties of GeSe and SnSe single crystals. Journal of the Korean Physical Society 72, 238–242 2018.

[3] Becke. A.D "Density-Functional Thermochemistry. The Role of exact Exchange." J. Chem. Phys. , 98, 5648, 1993.

[4] Becke, A. D. Density-functional thermochemistry. III. The role of exact exchange. J. Chem. Phys. 98, 56485652, 1993.

[5] Lee, C.; Yang, W.; Parr, R. G. Development of the Colle Salvetti correlation-energy formula into a functional of the electron density. Phys. Rev. B: Condens. Matter Mater. Phys. 37, 785789, 1988.

[6] Heyd, J.; Scuseria, G. E.; Ernzerhof, M. Erratum: "Hybrid functionals based on a screened Coulomb potential" J. Chem. Phys. , 124, 219906, 2006.

[7] Grimme, S. Semiempirical GGA-Type Density Functional Constructed with a Long-Range Dispersion Correction. J. Comput. Chem. 27, 17871799, 2006.

[8] Bucko, T.; Hafner, J.; Lebe gue, S.; A ngyan, J. G. Improved Description of the Structure of Molecular and Layered Crystals: Ab Initio DFT Calculations with Van der Waals Corrections. J. Phys. Chem. A 114, 1181411824,2010.

[9] Birch, F. Elasticity and constitution of the Earth's interior. J. Geophys. Res. 57, 227286, 1952.

[10] Dong-Kyun Seo and Roald Homann "Direct and indirect band gap types in one-dimensional conjugated or stacked organic materials" Theor. Chem. Acc. 102, 23-32 1999

[11] CRYSTAL 17. User's Manual September 18. R. Dovesi, V.R. Saunders, C. Roetti, R. Orlando, C. M. Zicovich-Wilson, F. Pascale, B. Civalleri, K.Doll, N.M. Harrison, I.J. Bush, Ph. D'Arco, M.Llunel, M. Causà, Y. Noël, L. Maschio, A. Erba, M.Rérat, S. Casassa. 2017

[12] http://www.crystalimpact.com/diamond/Default.html

[13] Vibrational and thermodynamic properties of GeSe in the quasiharmonic approximation. Volker L. Deringer, Ralf P. Stoffel, and Richard Dronskowski. Phys. Rev. B 89, 094303 2014

[14] Necessary and sufficient elastic stability conditions in various crystal systems Félix Mouhat and François-Xavier Coudert Phys. Rev. B 90, 224104, 2014

[15] Wu, Z.-j.; Zhao, E.-j.; Xiang, H.-p.; Hao, X.-f.; Liu, X.-j.; Meng, J. Crystal Structures and Elastic Properties of Superhard IrN2 and IrN3 from First Principles. Phys. Rev. B: Condens. Matter Mater. Phys. 76, 059904, 2007.

[16] Germanium Chalcogenide Thermoelectrics: Electronic Structure Modulation and Low Lattice Thermal Conductivity† Subhajit Roychowdhury, Manisha Samanta, Suresh Perumal, and Kanishka Biswas Chemistry of Materials 30 (17), 5799-5813, 2018

[17] Birch. F. "Finite Strain Isotherm And Velocities For Single-Crystal And Polycristalline NaCl At High-Pressures And 300-Degree-K." J. Geophys. Res. 83, 1257, 1978

[18] A. Erba, A. Mahmoud, D. Belmonte and R. Dovesi, J. Chem. Phys., 140, 124703 (2014)

[19] A.Kokalj "J.mol graph" Model. 17, 176-179 1999

[20] Bradley, C.J., Cracknell, A.P. and Author The mathematical theory of symmetry in solids. Oxford: Clarendon Press. 1972

11 Annex

182,003	25,816	35,201	0	0	0
-	166,019	68,397	0	0	0
-	-	100,576	0	0	0
-	-	-	97,72	0	0
-	-	-	-	53,178	0
-	-	-	-	-	43,246

Table 9: Elastic constants matrix for an Pnma crystal at 5 GPa

227,865	43,865	55,732	0	0	0
-	177,426	59,682	0	0	0
-	-	102,777	0	0	0
-	-	-	126,353	0	0
-	-	-	-	63,322	0
-	-	-	-	-	44,629

Table 10: Elastic constants matrix for an Pnma crystal at 10 GPa

271,996	51,644	64,979	0	0	0
-	217,973	84,395	0	0	0
-	-	141,432	0	0	0
-	-	-	153,954	0	0
-	-	-	-	74,882	0
-	-	-	-	-	47,466

Table 11: Elastic constants matrix for an Pnma crystal at 15 GPa

310,161	63,499	76,399	0	0	0
-	243,134	104,272	0	0	0
-	-	186,678	0	0	0
-	-	-	180,584	0	0
-	-	-	-	84,473	0
-	-	-	-	-	47,655

Table 12: Elastic constants matrix for an Pnma crystal at 20 GPa

395,317	39,532	79,946	0	0	0
-	302,096	148,553	0	0	0
-	-	247,386	0	0	0
-	-	-	226,159	0	0
-	-	-	-	82,856	0
-	-	-	-	-	65,592

Table 13: Elastic constants matrix for an Pnma crystal at 25 GPa

433,173	48,2	81,823	0	0	0
-	328,825	165,415	0	0	0
-	-	292,931	0	0	0
-	-	-	249,232	0	0
-	-	-	-	89,123	0
-	-	-	-	-	77,955

Table 14: Elastic constants matrix for an Pnma crystal at 30 GPa

Volume (A3)	P (GPa)	E (au)	G (au)	AE	AG
181.46	-1.00	-9792.4077	-9792.4494	0	0
171.75	-0.00	-9792.4090	-9792.4090	0	0
166.99	1.00	-9792.4085	-9792.3702	0	0
163.84	2.00	-9792.4075	-9792.3323	0	0
161.50	3.00	-9792.4061	-9792.2950	0	0
159.64	4.00	-9792.4046	-9792.2582	0	0
158.10	5.00	-9792.4031	-9792.2217	0	0
156.79	6.00	-9792.4014	-9792.1856	0	0
155.65	7.00	-9792.3997	-9792.1498	0	0
154.64	8.00	-9792.3980	-9792.1142	0	0
153.73	9.00	-9792.3962	-9792.0789	0	0
152.91	10.00	-9792.3944	-9792.0437	0	0
152.17	11.00	-9792.3926	-9792.0087	0	0
151.48	12.00	-9792.3908	-9791.9739	0	0
150.84	13.00	-9792.3890	-9791.9392	0	0
150.25	14.00	-9792.3872	-9791.9047	0	0
149.70	15.00	-9792.3853	-9791.8703	0	0
149.18	16.00	-9792.3835	-9791.8360	0	0
148.69	17.00	-9792.3816	-9791.8018	0	0
148.23	18.00	-9792.3798	-9791.7678	0	0
147.79	19.00	-9792.3779	-9791.7338	0	0
147.37	20.00	-9792.3761	-9791.7000	0	0
146.98	21.00	-9792.3742	-9791.6662	0	0
146.60	22.00	-9792.3723	-9791.6326	0	0
146.24	23.00	-9792.3705	-9791.5990	0	0
145.89	24.00	-9792.3686	-9791.5655	0	0
145.56	25.00	-9792.3667	-9791.5321	0	0
145.24	26.00	-9792.3649	-9791.4987	0	0
144.94	27.00	-9792.3630	-9791.4654	0	0
144.64	28.00	-9792.3611	-9791.4322	0	0
144.35	29.00	-9792.3593	-9791.3991	0	0
144.08	30.00	-9792.3574	-9791.3660	0	0

Table 15: EOS for Pnma structure

Volume (A3)	P (GPa)	E (au)	G (au)	2*G	AG	2*E	AE
46.26	-2	-4896.0420	-4896.0633	-9792.1265	-	-9792.0841	-
46.38	-1	-4896.0420	-4896.0526	-9792.1053	9.3585	-9792.0840	8.8054
46.5	0	-4896.0420	-4896.0420	-9792.0840	8.8410	-9792.0840	8.8413
46.62	1	-4896.0420	-4896.0313	-9792.0626	8.3666	-9792.0840	8.8269
46.75	2	-4896.0420	-4896.0206	-9792.0412	7.9178	-9792.0841	8.7957
46.88	3	-4896.0421	-4896.0099	-9792.0197	7.4872	-9792.0842	8.7554
47.01	4	-4896.0422	-4895.9991	-9791.9982	7.0715	-9792.0845	8.7092
47.15	5	-4896.0424	-4895.9883	-9791.9766	6.6679	-9792.0847	8.6584
47.29	6	-4896.0425	-4895.9775	-9791.9549	6.2749	-9792.0851	8.6039
47.43	7	-4896.0428	-4895.9666	-9791.9332	5.8914	-9792.0855	8.5459
47.58	8	-4896.0430	-4895.9557	-9791.9114	5.5163	-9792.0860	8.4848
47.74	9	-4896.0433	-4895.9448	-9791.8896	5.1491	-9792.0866	8.4205
47.9	10	-4896.0437	-4895.9338	-9791.8676	4.7891	-9792.0873	8.3532
48.06	11	-4896.0441	-4895.9228	-9791.8456	4.4361	-9792.0881	8.2827
48.23	12	-4896.0445	-4895.9118	-9791.8235	4.0897	-9792.0890	8.2090
48.41	13	-4896.0450	-4895.9007	-9791.8014	3.7494	-9792.0900	8.1319
48.59	14	-4896.0456	-4895.8896	-9791.7791	3.4154	-9792.0912	8.0512
48.78	15	-4896.0462	-4895.8784	-9791.7568	3.0871	-9792.0924	7.9666
48.98	16	-4896.0469	-4895.8672	-9791.7344	2.7647	-9792.0938	7.8779
49.19	17	-4896.0477	-4895.8559	-9791.7118	2.4480	-9792.0954	7.7847
49.41	18	-4896.0486	-4895.8446	-9791.6892	2.1370	-9792.0972	7.6865
49.64	19	-4896.0496	-4895.8333	-9791.6665	1.8315	-9792.0991	7.5828
49.88	20	-4896.0507	-4895.8218	-9791.6437	1.5315	-9792.1013	7.4730
50.14	21	-4896.0519	-4895.8104	-9791.6207	1.2374	-9792.1038	7.3563
50.41	22	-4896.0532	-4895.7988	-9791.5977	0.9489	-9792.1065	7.2316
50.71	23	-4896.0548	-4895.7872	-9791.5745	0.6662	-9792.1095	7.0979
51.03	24	-4896.0565	-4895.7756	-9791.5512	0.3898	-9792.1130	6.9532
51.38	25	-4896.0585	-4895.7638	-9791.5277	0.1195	-9792.1169	6.7955
51.77	26	-4896.0607	-4895.7520	-9791.5040	-0.1442	-9792.1214	6.6216
52.2	27	-4896.0634	-4895.7401	-9791.4802	-0.4008	-9792.1267	6.4268
52.71	28	-4896.0665	-4895.7281	-9791.4561	-0.6497	-9792.1331	6.2035
53.31	29	-4896.0705	-4895.7159	-9791.4318	-0.8899	-9792.1410	5.9379
54.09	30	-4896.0758	-4895.7036	-9791.4072	-1.1199	-9792.1516	5.5993

Table 16: EOS for CmCm structure

Volume (A3)	P (GPa)	E (au)	G (au)	4*G (eV)	AG	4*E (eV)	AE
42.96	-2	-2448.1025	-2448.1222	-9792.4888	0.0000	-9792.4100	0.0000
42.33	-1	-2448.1027	-2448.1124	-9792.4497	-0.0100	-9792.4109	-0.0857
41.75	0	-2448.1028	-2448.1028	-9792.4112	-0.0579	-9792.4112	-0.0579
41.21	1	-2448.1027	-2448.0933	-9792.3731	-0.0783	-9792.4109	-0.0649
40.71	2	-2448.1026	-2448.0839	-9792.3355	-0.0877	-9792.4102	-0.0750
40.23	3	-2448.1023	-2448.0746	-9792.2984	-0.0924	-9792.4091	-0.0818
39.79	4	-2448.1019	-2448.0654	-9792.2617	-0.0955	-9792.4077	-0.0835
39.37	5	-2448.1015	-2448.0563	-9792.2254	-0.0989	-9792.4060	-0.0797
38.98	6	-2448.1010	-2448.0474	-9792.1894	-0.1035	-9792.4040	-0.0705
38.6	7	-2448.1004	-2448.0385	-9792.1539	-0.1101	-9792.4018	-0.0560
38.25	8	-2448.0998	-2448.0296	-9792.1186	-0.1191	-9792.3993	-0.0366
37.91	9	-2448.0992	-2448.0209	-9792.0837	-0.1307	-9792.3967	-0.0128
37.58	10	-2448.0985	-2448.0123	-9792.0490	-0.1453	-9792.3939	0.0152
37.28	11	-2448.0977	-2448.0037	-9792.0147	-0.1629	-9792.3909	0.0471
36.98	12	-2448.0969	-2447.9952	-9791.9806	-0.1835	-9792.3878	0.0824
36.7	13	-2448.0961	-2447.9867	-9791.9468	-0.2072	-9792.3845	0.1210
36.43	14	-2448.0953	-2447.9783	-9791.9133	-0.2340	-9792.3812	0.1626
36.17	15	-2448.0944	-2447.9700	-9791.8800	-0.2639	-9792.3777	0.2070
35.92	16	-2448.0935	-2447.9617	-9791.8469	-0.2968	-9792.3741	0.2539
35.67	17	-2448.0926	-2447.9535	-9791.8141	-0.3327	-9792.3705	0.3031
35.44	18	-2448.0917	-2447.9454	-9791.7815	-0.3715	-9792.3667	0.3546
35.22	19	-2448.0907	-2447.9373	-9791.7490	-0.4133	-9792.3629	0.4080
35	20	-2448.0898	-2447.9292	-9791.7168	-0.4580	-9792.3590	0.4633
34.79	21	-2448.0888	-2447.9212	-9791.6848	-0.5054	-9792.3551	0.5203
34.58	22	-2448.0878	-2447.9132	-9791.6530	-0.5557	-9792.3511	0.5790
34.39	23	-2448.0867	-2447.9053	-9791.6214	-0.6086	-9792.3470	0.6391
34.19	24	-2448.0857	-2447.8975	-9791.5899	-0.6641	-9792.3429	0.7006
34.01	25	-2448.0847	-2447.8897	-9791.5586	-0.7223	-9792.3387	0.7634
33.83	26	-2448.0836	-2447.8819	-9791.5275	-0.7830	-9792.3345	0.8274
33.65	27	-2448.0825	-2447.8741	-9791.4965	-0.8461	-9792.3302	0.8926
33.48	28	-2448.0815	-2447.8664	-9791.4657	-0.9117	-9792.3259	0.9588
33.32	29	-2448.0804	-2447.8588	-9791.4351	-0.9797	-9792.3216	1.0260
33.16	30	-2448.0793	-2447.8512	-9791.4046	-1.0501	-9792.3172	1.0941

Table 17: EOS for Fm-3m structure